General Circulation Model Sensitivity of Globally Averaged Albedo and Outgoing Longwave Radiation to Ice Crystal Shape

D. L. Mitchell
Desert Research Institute
Reno, Nevada

J. M. Edwards
Hadley Centre for Climate Prediction and Research, Meteorological Office
Bracknell, United Kingdom

P. N. Francis
Meteorological Research Flight
Farnborough, United Kingdom

We will first demonstrate the sensitivity of cirrus radiative properties to ice crystal shape by reformulating a recent treatment of radiative properties (Mitchell et al. 1996c) in terms of an effective diameter, D_e. We then show what impact crystal shape has in general circulation model (GCM) simulations.

Effective Diameter

Our definition of effective diameter is essentially the same concept as the Foot definition of effective radius (Francis 1994), which has been shown to predict shortwave (SW) and longwave (LW) fluxes in cirrus, based on observed microphysics, in reasonable agreement with observed fluxes (Francis 1994). We use effective diameter instead of radius because this simplifies the definition somewhat:

$$D_e = \frac{IWC}{\rho_i P_t} \tag{1}$$

where IWC = ice water content
ρ_i = density of bulk ice (which refractive indexes are referenced to)
P_t = size distribution projected area.

If we define the ice particle size distribution as

$$N(D) = N_o D^\nu \exp(-\lambda D) \tag{2}$$

where D = ice particle maximum dimension

and define ice particle mass and projected area as

$$m = \alpha D^\beta \tag{3}$$

$$P = \sigma D^\delta \tag{4}$$

then Equation 1 can be expressed quantitatively. However, it is critical to account for the fact that Equation 3 and sometimes Equation 4 change for a given crystal type near $D = 100$ μm. This can be done by expressing D_e in terms of the incomplete gamma function:

$$D_e = \frac{\dfrac{\alpha_1 \gamma(\beta_1+\nu+1,D_o\lambda)}{\lambda^{\beta_1+\nu+1}} + \dfrac{\alpha_2 \Gamma(\beta_2+\nu+1,D_o\lambda)}{\lambda^{\beta_2+\nu+1}}}{\dfrac{\sigma_1 \gamma(\delta_1+\nu+1,D_o\lambda)}{\lambda^{\delta_1+\nu+1}} + \dfrac{\delta_2 \Gamma(\sigma_2+\nu+1,D_o\lambda)}{\lambda^{\delta_2+\nu+1}}} \tag{5}$$

where $D_o = 100$ μm
"1" subscripts refer to crystals $\leq D_o$
"2" subscripts crystals $> D_o$
γ denotes the small gamma function
Γ denotes the large gamma function
(Abramowitz and Stegun 1965).

The extinction coefficient can now be expressed as

$$\beta_{ext} = \frac{2\ IWC}{\rho_i D_e} \tag{6}$$

while the absorption coefficient is

$$\beta_{abs} = \overline{Q}_{ab} P_t \tag{7}$$

where $\overline{Q}_{abs}$ is the absorption efficiency representative of the entire size distribution. In the thermal IR, $\overline{Q}_{abs}$ can be expressed in terms of D_e (Mitchell et al. 1996b, 1996c):

$$\overline{Q}_{abs} = 1 - \exp(-4\pi n_i D_e \Lambda) \qquad (8)$$

where n_i = imaginary refractive index
Λ = wavelength.

In the near infrared (IR), the slightly more complex expression in Mitchell (1996c) can be used, which accounts for internal reflection and refraction. Values of the mass and area constants used in Equation 5 are reported in Mitchell (1996c).

Size spectra are treated as bimodal (Mitchell et al. 1996a), being a composite of a small particle (D < 100 μm) exponential distribution, $N_s(D)$, and a larger particle gamma distribution, $N_l(D)$. Examples are given in Figure 1, where the mean D for $N_l(D)$, $\overline{D}$, was 100 μm and 200 μm, respectively. The values of v was 2 for $\overline{D}$ = 200 μm, but decreases to 0 for $\overline{D}$ < about 50 μm, as predicted by the expression:

$$v = v_{max}\{1 - \exp[-(\overline{D}/k\underline{D}_s)^3]\} \qquad (9)$$

where $v_{max} = 2$, k and $\overline{D}_s$ are 2.5 and 40 μm for polycrystals ($\overline{D}_s$ pertains to $N_s(D)$) and 5.0 and 20 μm for other crystal
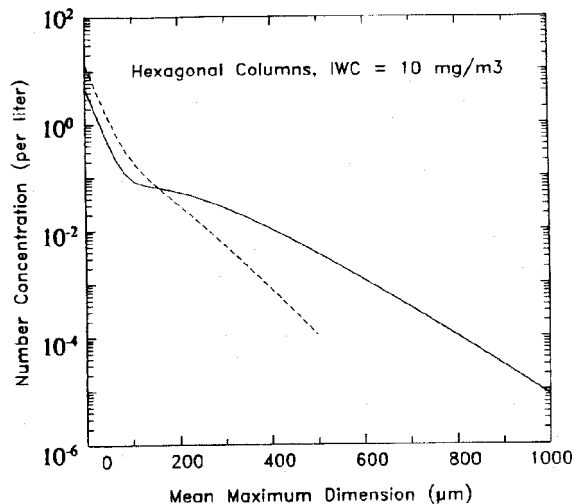
Figure 1. Examples of bimodal size spectra predicted by the radiation scheme for $\overline{D}$ = 100 μm (dashed) and 200 μm (solid).

shapes, based on *limited* ice crystal replicator measurements (Mitchell 1996a). Numerous ice spectra from 2D-C probes indicate bimodal behavior generally vanishes when $\overline{D}$ < 50 μm.

Using this formulation of v, D_e is plotted against $\overline{D}$ for different crystal types in Figure 2. It is seen that D_e may vary by more than a factor of 2 for a given $\overline{D}$. Similar results were obtained for exponential spectra. If the D_e dependence on Equations 3 and 4 was based on large crystals only (D > 100 μm), D_e would be grossly overestimated for D < 50 μm. It was also found that D_e may vary by up to 50% or more because of changes in v. Thus, D_e is sensitive to both crystal shape and size distribution shape.
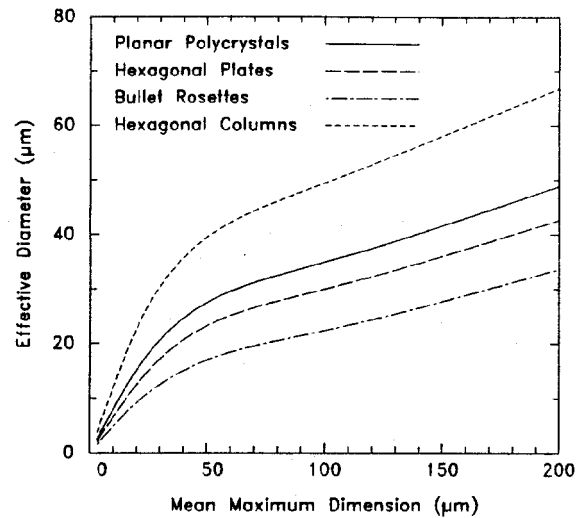
Figure 2. Dependence of D_e on ice crystal shape over a range of $\overline{D}$.

Also, for monomodal size spectra, the albedo, absorptivity, and emissivity predicted by the above D_e approach are virtually identical to those predicted by the scheme in Mitchell et al. (1996c). This is because both schemes are based on the concept of an "effective photon path" through an ice crystal, defined as

$$d_e = \text{ice crystal volume/projected area.}$$

The difference in this work is that a size distribution value for d_e was found, D_e, which was taken outside the integrals for β_{ext} and β_{abs}. However, cirrus radiative properties predicted for bimodal size spectra do differ significantly from those predicted for monomodal spectra having the same $\overline{D}$.

General Circulation Model Calculations

The cirrus radiation treatment described in Mitchell (1996c) was incorporated into the Hadley Centre's GCM, known as the Unified Model (UM), and was based on bimodal size spectra as described here. Based on numerous measurements of ice particle size spectra (e.g., Ryan 1996; Knollenburg et al. 1993; McFarquhar and Heymsfield 1996), the following temperature dependence for $\overline{D}$ was used:

$$\overline{D} = \exp(0.05522(T-6.5))/9.702 \qquad (10)$$

where T is in °C. Equation 10 was tuned to conform to 2D-C probe measurements (as opposed to 2D-P size spectra). The Edwards-Slingo (1996) radiation transfer scheme, which treats scattering in the thermal IR, was used. The single scattering albedo, asymmetry parameter, and mass extinction coefficient were parameterized with polynomial fits as functions of $\overline{D}$.

To determine initial radiative forcings associated with different crystal shapes, the UM was run for one time-step with a single crystal shape representing the ice phase. Ice spheres of 30-μm diameter, the UM's standard ice phase representation, were also used and contrasted. Hexagonal columns were most similar to ice spheres, while bullet rosettes were least similar, and all crystal types reflected more SW radiation than ice spheres. As shown in Figure 3, the globally averaged, instantaneous (one time-step) difference in reflected SW radiation between a "simulation" assuming bullet rosette ice crystals and that assuming hexagonal columns was 9.3 Wm^{-2}. This translates to a 3% increase in mean global albedo (rosettes are brightest). The corresponding difference for outgoing LW radiation (OLR) was -4.7 Wm^{-2}, giving a net difference of 4.6 Wm^{-2}. This compares to a net global forcing due to a CO_2 doubling of about 4 Wm^{-2}. Differences in zonal mean reflected SW and OLR values between simulations assuming rosettes and ice spheres are shown in Figure 4. While mean OLR differences are similar to rosettes minus columns, columns appear brighter than spheres by about 1.8 Wm^{-2}.

This high sensitivity of the global radiation balance to ice crystal shape is largely manifested through the dependence of D_e on crystal shape. These results would be modified somewhat in a multi-year simulation. Nonetheless, they are dramatic enough to indicate that we not only need to represent clouds
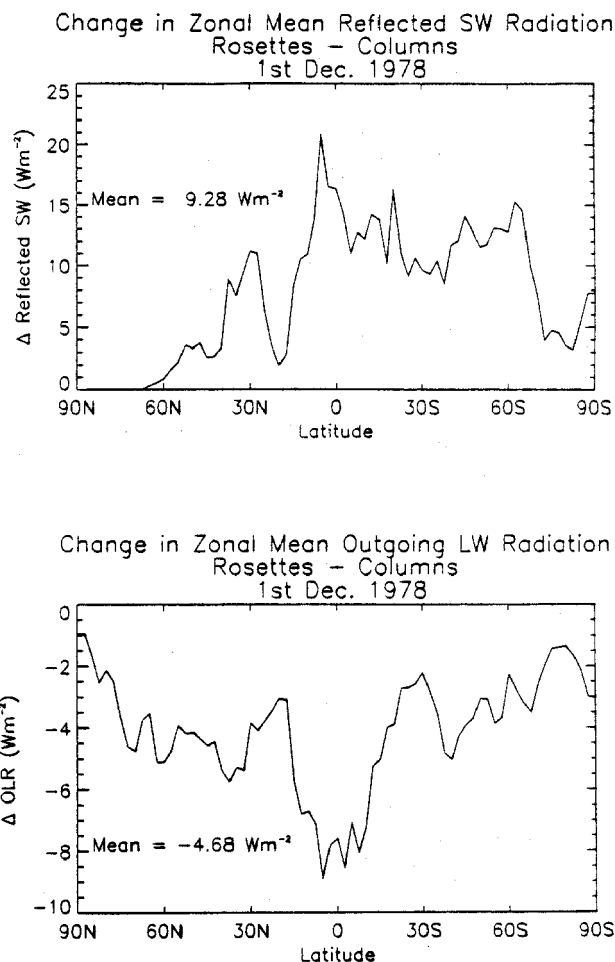
Figure 3. Changes in zonal means of reflected SW and outgoing LW radiation due to changing the ice phase from hexagonal columns to bullet rosettes.

adequately in GCMs, but also need to understand what factors determine crystal shape in ice clouds if climate is to be reliably predicted.

Finally, a 15-month UM simulation using planar polycrystals resulted in warming the upper tropical troposphere by about 1.0K, reducing the UM's cold bias there. Better agreement with Earth Radiation Budget Experiment (ERBE) data was found for SW and possibly LW fluxes relative to 30-μm ice spheres.

Acknowledgment

Change in Zonal Mean Reflected SW Radiation
Rosettes − 30 μm−spheres
1st Dec. 1978

Mean = 11.06 Wm⁻²

Change in Zonal Mean Outgoing LW Radiation
Rosettes − 30 μm−spheres
1st Dec. 1978

Mean = −4.55 Wm⁻²
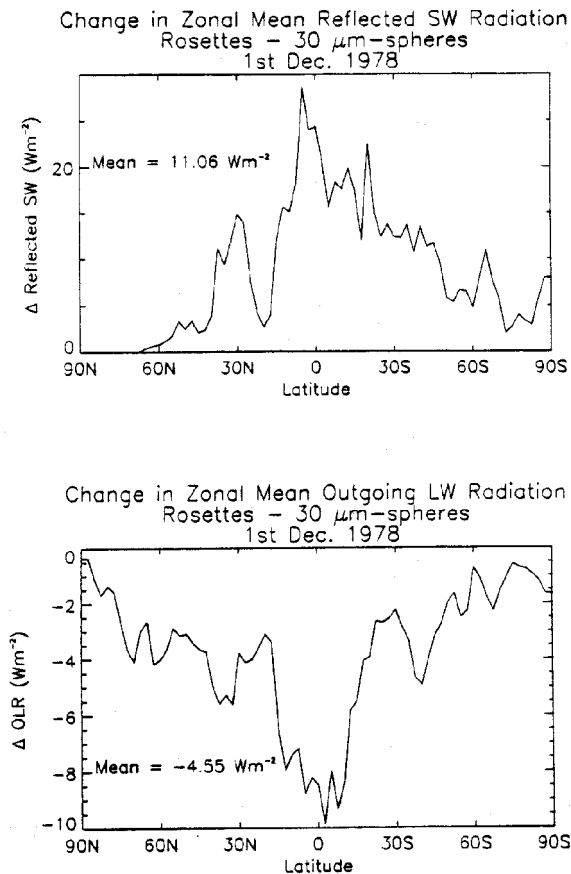
Figure 4. Changes in zonal means of reflected SW and outgoing LW radiation due to changing the ice phase in the UM from 30-μm ice spheres to bullet rosettes.

References

Abramowitz, M., and I. A. Stegun, 1965: *Handbook of Mathematical Functions.* Dover.

Edwards, J. M., and A. Slingo, 1996: Studies with a flexible new radiation code. I: Choosing a configuration for a large-scale model. *Q.J.R. Meteorol. Soc.*, **122**, 689-719.

Francis, P. N., A. Jones, R. W. Saunders, K. P. Shine, A. Slingo, and Zhian Sun, 1994: An observational and theoretical study of the radiative properties of cirrus: Some results from ICE '89. *Q.J.R. Meteorol. Soc.*, **120**, 809-848.

Knollenburg, R. G., K. Kelly, and J. C. Wilson, 1993: Measurements of high number densities of ice crystals in the tops of tropical cumulonimbus. *J. Geophys. Res.*, **98**, 8639-8664.

McFarquhar, G. M., and A. J. Heymsfield, 1996: Microphysical characteristics of three anvils sampled during the Central Equatorial Pacific Experiment (CEPEX). *J. Atmos. Sci.*, **53**, 2401-2423.

Mitchell, D. L., S. K. Chai, Y. Liu, A. J. Heymsfield, and Y. Dong, 1996a: Modeling cirrus clouds. Part I: Treatment of bimodal size spectra and case study analysis. *J. Atmos. Sci.*, **53**, 2952-2966.

Mitchell, D. L., D. Koracin, and E. Carter, 1996b: Radiative properties of ice clouds. *Proceedings of the Fifth Atmospheric Radiation Measurement (ARM) Science Team Meeting.* March 19-23, 1995, San Diego, California, pp. 215-217. CONF-9503140, U.S. Department of Energy, Washington, D.C.

Mitchell, D. L., A. Macke, and Y. Liu, 1996c: Modeling Cirrus Clouds. Part II: Treatment of Radiative Properties. *J. Atmos. Sci.*, **53**, 2967-2988.

Ryan, B. F., 1996: On the global variation of precipitating layer clouds. *Bull. Amer. Meteorol. Soc.*, **77**, 53-70.